Electron- and muon-neutrino content of the atmospheric flux

R. Becker-Szendy,[d] C. B. Bratton,[c] D. Casper,[a] S. T. Dye,[a] W. Gajewski,[e] M. Goldhaber,[b] T. J. Haines,[g] P. G. Halverson,[e] D. Kielczewska,[e,i] W. R. Kropp,[e] J. G. Learned,[d] J. M. LoSecco,[h] S. Matsuno,[e] G. McGrath,[d] C. McGrew,[e] R. Miller,[f] L. R. Price,[e] F. Reines,[e] J. Schultz,[e] H. W. Sobel,[e] J. L. Stone,[a] L. R. Sulak,[a] and R. Svoboda[f]

[a]*Boston University, Boston, Massachusetts 02215*
[b]*Brookhaven National Laboratory, Upton, New York 11973*
[c]*Cleveland State University, Cleveland, Ohio 44115*
[d]*The University of Hawaii, Honolulu, Hawaii 96822*
[e]*The University of California at Irvine, Irvine, California 92717*
[f]*Louisiana State University, Baton Rouge, Louisiana 70803-4001*
[g]*The University of Maryland, College Park, Maryland 20742*
[h]*University of Notre Dame, Notre Dame, Indiana 46556*
[i]*Warsaw University, Warsaw, Poland*

(Received 19 March 1992)

Neutrino interactions from a 7.7 kton yr exposure of the IMB-3 detector are analyzed. A total of 935 contained events radiating over ~ 50 MeV of Čerenkov-equivalent energy and consistent with atmospheric neutrino interactions are identified. Of these, 610 have a single Čerenkov ring. Single-ring interactions are efficiently separated into those containing a showering particle (produced mainly by ν_e) and those containing a nonshowering particle (produced mainly by ν_μ). In the momentum range $100 < p_e < 1500$ MeV/c and $300 < p_\mu < 1500$ MeV/c, the fraction of nonshowering events is $0.36 \pm 0.02(\text{stat}) \pm 0.02(\text{syst})$. Based on detailed models of neutrino production and interaction, a fraction of $0.51 \pm 0.01(\text{stat}) \pm 0.05(\text{syst})$ is expected. This deficit of nonshowering, or excess of showering, events relative to the total is supported by an independent analysis of muon decay signals. In the same sample $33 \pm 2(\text{stat})\%$ of events are accompanied by one or more muon decays, while $43 \pm 1(\text{stat})\%$ are expected. Further studies that could reduce systematic errors and discover the cause of these discrepancies are suggested.

PACS number(s): 96.40.Tv, 95.85.Qx

Nearly isotropic fluxes of ν_e and ν_μ are produced over a broad range of energies by cosmic-ray interactions with the atmosphere. Because of uncertainties in the primary cosmic-ray flux and models of hadron interactions with air, the absolute numbers of ν_e and ν_μ can be predicted only to within $\pm 20\%$. The ratio of the two flavors, which is independent of flux, is predicted with more certainty ($\pm 5\%$) [1–3]. Interactions of atmospheric neutrinos are recorded in underground detectors and constitute the dominant background to the search for nucleon decay. A majority of the interactions result from charged-current quasielastic neutrino-nucleon scattering, producing a single charged muon or electron. The ν_μ content of the atmospheric neutrino flux is thus approximated by the fraction of events containing a muon decay signal. A smaller than expected fraction was observed in the earlier IMB-1 experiment [4]. Applying particle-identification techniques to selected single-particle events permits an independent, more reliable estimate of the flavor content of the atmospheric neutrino flux. Simulations of neutrino interactions at the relevant energies indicate strong correlations between ν_e-induced (ν_μ-induced) events and "electronlike" or "showering" ("muonlike" or "nonshowering") particles. A smaller than expected ratio of nonshowering events to the total has been reported previously by Kamiokande [5] and IMB-3 [6,7]. Similar discrepancies, found in the final data set of the IMB-3 experiment, are reported here.

The IMB-3 detector is an 8-kton water Čerenkov detector located at a depth of 1570 meters of water equivalent (mwe) (600 m) in the Morton Salt mine near Cleveland, Ohio. It consists of a tank of water (18 m $\times$ 17 m $\times$ 22.5 m) instrumented on all six faces with 2048×20 cm photomultiplier tubes (PMT's). Details of the construction, operation, and calibration of the detector are available elsewhere [7,8]. The trigger threshold is ~ 15 MeV of Čerenkov equivalent, or visible, energy. Visible energy is measured using the number of photoelectrons collected in the recorded event. It is defined as the energy of an electron which would produce the same number of Čerenkov photons. One photoelectron corresponds to approximately 1 MeV of visible energy. The visible energy resolution is $3\%\ [E_{\text{vis}}(\text{GeV})]^{-1/2}$, plus a constant systematic term of $\pm 7\%$. Atmospheric muons, entering the detector from above, comprise the vast majority of recorded events. The 2.5×10^5 entering-muon triggers per day are vetoed by reconstruction of their Čerenkov rings, leaving the few contained events per day for fur-

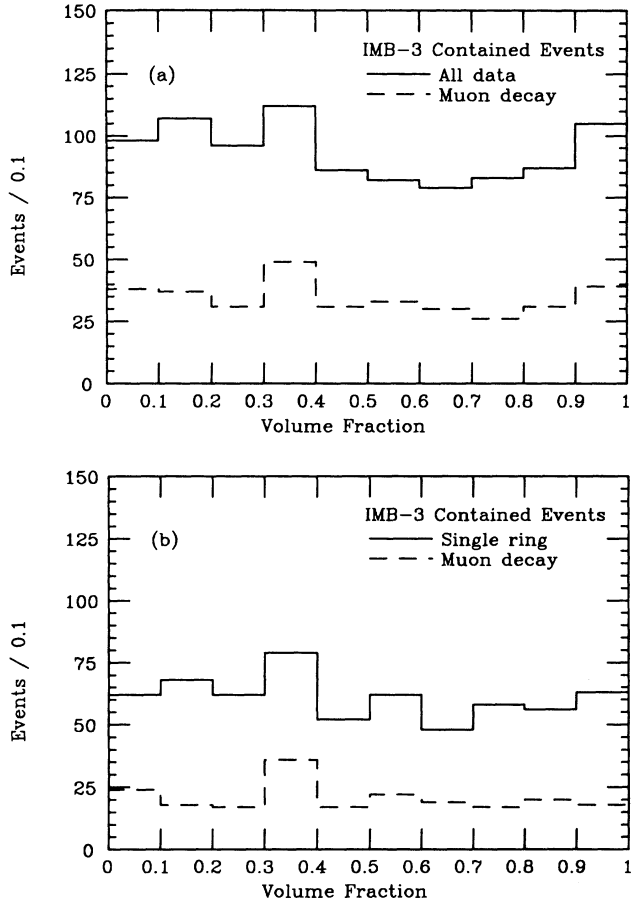

FIG. 1. (a) Fiducial volume distribution of all contained events and those with a muon decay. (b) Fiducial volume distribution of single-ring events and those with a muon decay.

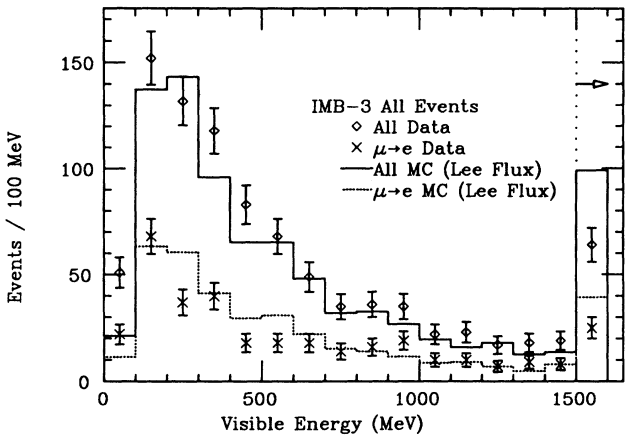

FIG. 2. Visible energy of all contained events and those with a muon decay.

ther study.

For this study, a 3.3-kton fiducial mass was used as target for atmospheric neutrinos. Detector triggers resulting from prompt firing of 70–900 PMT's were analyzed separately by two subgroups using independently developed calibrations and event filters. The 70-PMT lower limit corresponds to roughly 50 MeV of visible energy. A sample of events originating inside the fiducial volume was constructed from the results of both analyses. The combined efficiency for recovering contained events, assuming the filtering inefficiencies were independent, was 93%. A total of 935 events within the N_{PMT} cut were identified in data collected between May 1986 and March 1991, corresponding to a total exposure of 7.7

TABLE I. Results of the nonshowering/showering voting for the 851-*d* IMB-3 contained data and the simulated atmospheric neutrino data.

	Data		Simulation (Ref. [1])	
	3-vote	2-vote	3-vote	2-vote
Single ring in p cuts				
Unanimous	289	90	316.4	78.2
Split decision	110	18	116.6	14.1
Showering				
Unanimous	190	68	148.5	50.5
Split decision	60	7	55.3	6.6
Nonshowering				
Unanimous	99	22	167.9	27.7
Split decision	50	11	61.3	7.5
All single ring				
Unanimous	309	118	336.8	109.0
Split decision	140	43	134.8	31.8
Showering				
Unanimous	201	85	155.7	68.2
Split decision	78	14	58.8	9.0
Nonshowering				
Unanimous	108	33	181.1	40.8
Split decision	62	29	76.0	22.8

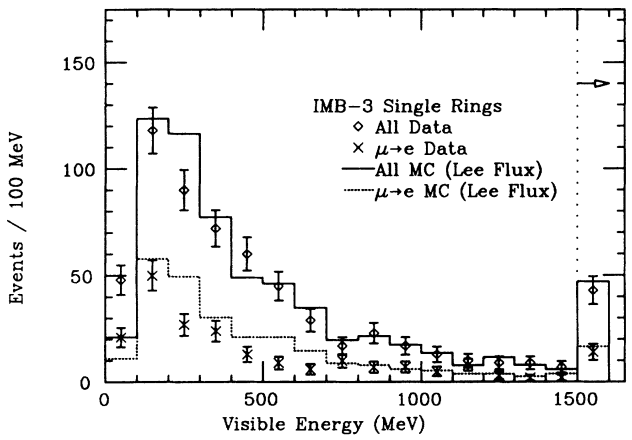

FIG. 3. Visible energy of single-ring events and those with a muon decay.

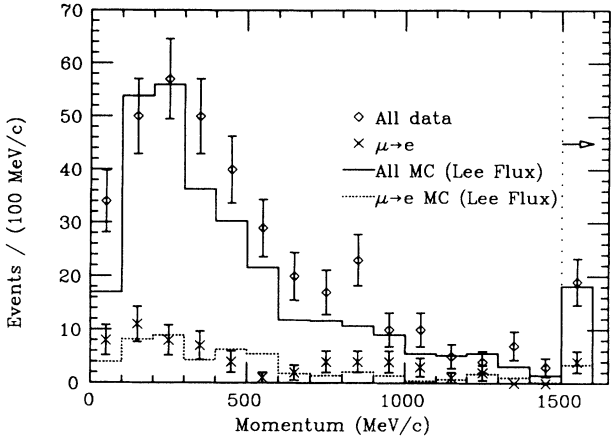

FIG. 4. Momentum of single-ring showering events and those with a muon decay.

kton yr. Each event was scanned visually to determine the vertex, and the number and direction of Čerenkov rings present. This procedure identified 610 events with a single ring and 325 with multiple rings. By searching for coincidences among PMT's firing after the trigger, muon decay electrons were detected with greater than 80% efficiency and contamination of only 2%. In the single-ring (multiple-ring) sample, 208 (137) events were accompanied by at least one muon decay signal.

Simple tests can be performed to estimate the purity of the sample. The numbers of contained events, and those with a muon decay, identified in equal fractions of the fiducial volume are presented in Fig. 1(a). Corresponding distributions for single-ring events are displayed in Fig. 1(b). Contamination from atmospheric muons, if present, would be manifest as an excess of events with a muon decay at the edge of the fiducial volume. Uniform distributions, which are expected from interactions of atmospheric neutrinos, are observed in the data. No contamination from atmospheric muons is apparent.

The physics capabilities of a large water Čerenkov detector are greatly extended through particle identification. A reliable means of discriminating between particle types is provided by measuring the geometry and intensity distribution of Čerenkov hit patterns. Diffuse showering patterns are associated with $e^{\pm}$ and γ, while sharper, nonshowering patterns are associated with $\mu^{\pm}$, $\pi^{\pm}$, and p. Only single-ring events allow reliable determination of the parent neutrino flavor. Using three independent, automated identification algorithms, the single-ring events are classified as showering or nonshowering [7]. In most cases, the final classification is determined by a majority vote of the three tests: each test casts one vote. Because one test fails to classify some events, the identity of 26% of data events is determined by only two tests. In this subsample, the voting is unanimous for 73% of events. When the votes are split (7% of all single-ring events), the classification is made by the "more certain" result, based on quality factors calculated by the algorithms. Voting results for the particle identification tests are shown in Table 1 for both data and simulation. In the single-ring sample, 378 events are identified as showering and 232 as nonshowering.

To predict the showering and/or nonshowering composition and the muon decay content of the sample, a simulation of neutrino interactions in water [7] is combined with a three-dimensional model of atmospheric neutrino production [1] (including effects of muon polar-

TABLE II. Summary of the 851-*d* IMB-3 contained data and simulated atmospheric neutrino data.

	Data			Simulation (Ref. [1])		
	All	Muon decay	% muon decay	All	Muon decay	% muon decay
Single ring in p cuts	507	168	33±2	525.3	223.3	43±1
Showering	325	51	16±2	257.3	43.2	17±1
Nonshowering	182	117	64±4	268.0	180.1	67±1
All single ring	610	208	34±2	612.4	261.5	43±1
Showering	378	63	17±2	291.7	50.5	17±1
Nonshowering	232	145	63±3	320.7	211.0	66±1
Multiple ring	325	137	42±3	239.9	115.6	48±1
Total	935	345	37±2	852.4	377.6	44±1

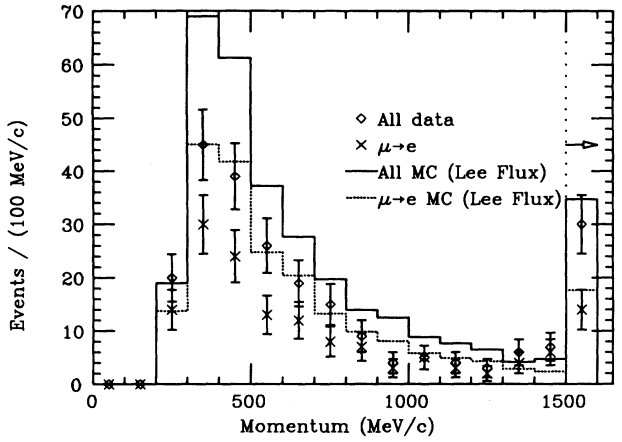

FIG. 5. Momentum of single-ring nonshowering events and those with a muon decay.

ization). Simulated interactions are then propagated through the detector Monte Carlo program and the data filtering and classification routines. An identical analysis has been performed on smaller sets of simulated data produced by two independent neutrino interaction and/or detector simulation packages. The performance of the identification algorithms does not depend on the particular neutrino physics model or detector response model which is used. Studies indicate the correlation between ν_e-induced (ν_μ-induced) events and identified single-ring showering (nonshowering) events is 87 ± 1(stat)% [92 ± 1(stat)%].

A summary of the 851 day IMB-3 contained data, and the simulated atmospheric neutrino data, is presented in Table II. Simulations using other atmospheric neutrino production models [2,3] yield event rates up to 30% higher than the prediction presented here. Ratios of various classes of events predicted by the other models are, however, indistinguishable from those presented here [6]. Several inconsistencies in the data are noted. The percentages of events with a muon decay and with a single Čerenkov ring are lower in the data than in the simulation. In the data, 37 ± 2(stat)% of all events are accompanied by a muon decay, while the simulation predicts 44 ± 1(stat)%. This inconsistency is more pronounced in the subsample of single-ring events, for which the fraction of events with a muon decay signal is 0.34 ± 0.02(stat), while a fraction of 0.43 ± 0.01(stat) is predicted. In addition, the fraction of single-ring events

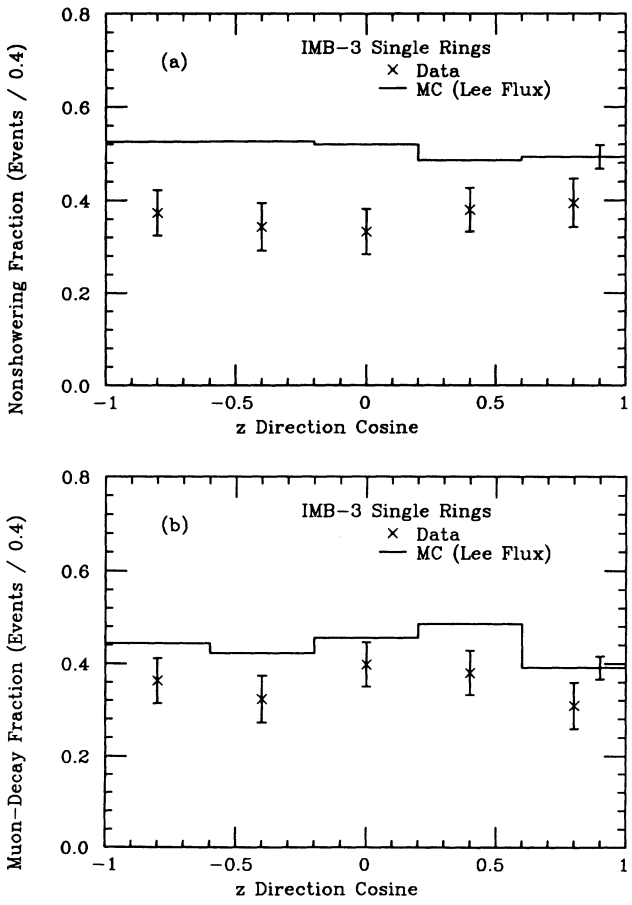

FIG. 6. (a) Nonshowering fraction vs zenith angle. (b) Muon-decay fraction vs zenith angle.

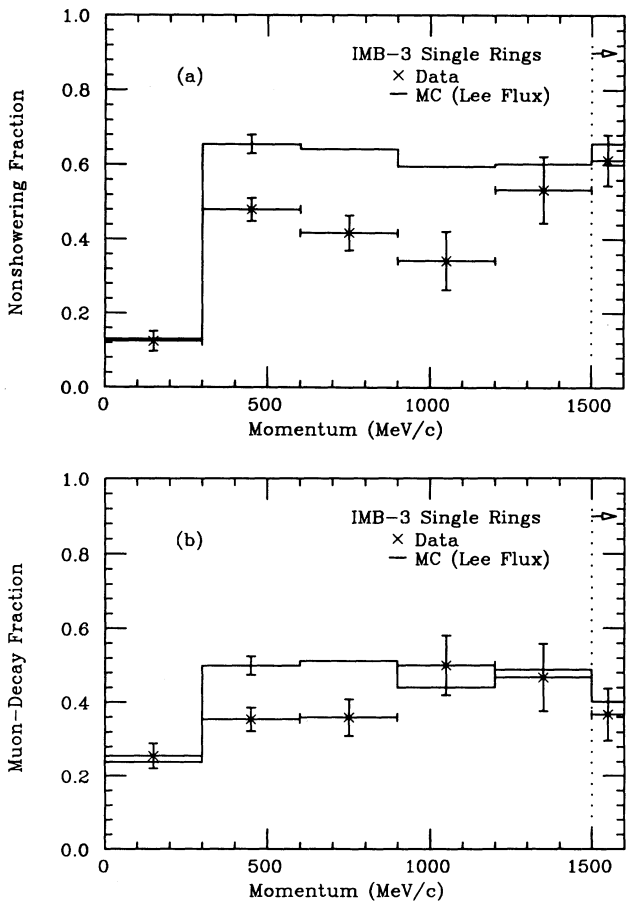

FIG. 7. (a) Nonshowering fraction vs momentum. (b) Muon-decay fraction vs momentum.

in the data is 0.65 ± 0.01(stat) compared with 0.72 ± 0.01(stat) in the simulation.

The visible-energy spectra of all events and muon-decay events are compared with the simulation in Fig. 2. The shapes of the spectra agree. The discrepancy between the measured and predicted spectra above 1500 MeV is limited to multiple-ring events, originating primarily from poorly understood multiple-pion production processes, and should not affect this study. Figure 3 demonstrates the agreement between the observed and expected spectra for single-ring events.

Discussion is now restricted to single-ring events. Momentum distributions for showering, and nonshowering events, along with their respective muon decay subsamples, are shown in Figs. 4 and 5. The shapes of the simulated spectra are well matched by the recorded data. Moreover, for both showering and nonshowering events, the expected and observed muon decay fractions agree. However, the observed ratio of nonshowering events to all single-ring events is lower than predicted. To further explore this inconsistency we focus our attention on the momentum ranges $100<p_e<1500$ MeV/c and $300<p_\mu<1500$ MeV/c; low-momentum events are excluded to increase the reliability of particle identification and high-momentum events are cut to veto exiting particles. In this range, nonshowering events comprise 36 ± 2(stat)±2(syst)% of the total. Based on the simulation, 51 ± 1(stat)±5(syst)% is expected. No time-dependent systematic drift of the nonshowering fraction is observed in the data. When statistical and systematic uncertainties are combined, the measured fraction of nonshowering single-ring events within the momentum cuts is 2.6σ below expectation. The observed fraction of events with muon decays, independent of particle identification algorithms, is $4.0\sigma_{\text{stat}}$ below expectation. Because of the uncertainty in the absolute flux, it is difficult to determine if these discrepancies represent a deficit of nonshowering events, an excess of showering events, or a combination of the two.

Atmospheric neutrinos interacting within the IMB-3 detector traverse distances of a few kilometers to 13 000 km from their points of origins in the atmosphere. This long base line translates to a sensitive window of 1 km/GeV $<L/E<10^5$ km/GeV for possible oscillation of neutrino flavor. Neutrino oscillations are a possible, though not necessary, explanation of the data. The overall spectra agree reasonably well with predictions (Figs. 2 and 3). The unexpected low fractions of nonshowering events and events with a muon decay seem independent of zenith angle [(see Figs. 6(a) and 6(b)] and momentum [see Figs. 7(a) and 7(b)]. Much of the range of L/E greater than 1 km/GeV is sampled by measurements of externally produced upward-going muons from higher energy neutrinos. Within errors, no oscillation effect is observed in those data [9,10].

At this point, systematic effects dominate the experimental errors in the measurement of the nonshowering event fraction. Experiments designed to reduce these systematic uncertainties could uncover the cause of the apparent ν_μ deficit (and/or ν_e excess). More precise measurements of muon and pion growth curves at high altitude would improve confidence in the neutrino production model. Cross-section measurements using a controlled neutrino beam on oxygen targets, or a calculation more realistic than the Fermi gas model but amenable to event simulation, would help to eliminate uncertainties in the neutrino interaction model. Exposing a test detector similar to IMB-3 to muons and electrons of appropriate energy from an accelerator would test the accuracy of particle identification.

In conclusion, the flavor composition of atmospheric neutrinos has been measured using two independent techniques: muon decays and particle identification. A deficit of muon neutrinos, or excess of electron neutrinos, compared with prediction has been observed. The Kamioka experiment has observed a remarkably similar effect [5]. Experiments and/or theoretical work to reduce systematic uncertainties are possible and could discover the cause of the apparent discrepancy.

The authors thank Morton International for accommodating the experiment in their Fairport mine. Special thanks are due to Joe Reese, Ted Darden, Eric Hazen, and Bob Render for technical support. This research was funded in part by the U.S. Department of Energy.

[1] H. Lee and Y. S. Koh, Nuovo Cimento **105B**, 883 (1990).
[2] S. Barr, T. K. Gaisser, S. Tilav, and P. Lipari, Phys. Lett. B **214**, 147 (1988); G. Barr, T. K. Gaisser, and T. Stanev, Phys. Rev. D **39**, 3532 (1989).
[3] M. Honda, K. Kasahara, K. Hidaka, and S. Midorikawa, Phys. Lett. B **248**, 193 (1990).
[4] T. J. Haines *et al.*, Phys. Rev. Lett. **57**, 1986 (1986).
[5] K. S. Hirata *et al.*, Phys. Lett. B **205**, 416 (1988); M. Takita, Ph.D. thesis, University of Tokyo, ICRR-Report No. 186-89-3, 1989; T. Kajita *et al.*, in *Proceedings of the Twenty-Fifth International Conference on High-Energy Physics,* Singapore, 1990, edited by K. K. Phua and Y. Yamaguchi (World Scientific, Singapore, 1991), p. 685; K. S. Hirata *et al.*, Phys. Lett. B **280**, 146 (1992).
[6] D. Casper *et al.*, Phys. Rev. Lett. **66**, 2561 (1991).
[7] D. Casper, Ph.D. thesis, University of Michigan, 1990.
[8] R. Becker-Szendy *et al.*, Boston University Report No. BUHEP-92-6, 1992 (unpublished).
[9] Y. Oyama, Ph.D. thesis, University of Tokyo, ICRR-Report No. 193-89-10, 1989; Y. Oyama *et al.*, Phys. Rev. D **39**, 1481 (1989).
[10] R. Becker-Szendy *et al.*, Phys. Rev. Lett. **69**, 1010 (1992).